Insect Biochemistry and Molecular Biology 115 (2019) 103245

Contents lists available at ScienceDirect

Insect Biochemistry and Molecular Biology

journal homepage: www.elsevier.com/locate/ibmb

Amine-binding properties of salivary yellow-related proteins in phlebotomine sand flies

Petra Sumova[a,*], Michal Sima[a], Barbora Kalouskova[b], Nikola Polanska[a], Ondrej Vanek[b], Fabiano Oliveira[c], Jesus G. Valenzuela[c], Petr Volf[a]

[a] Department of Parasitology, Faculty of Science, Charles University, Prague, Czech Republic
[b] Department of Biochemistry, Faculty of Science, Charles University, Prague, Czech Republic
[c] Vector Molecular Biology Section, Laboratory of Malaria and Vector Research, National Institute of Allergy and Infectious Diseases, National Institutes of Health, Rockville, MD, USA

ARTICLE INFO

Keywords:
Yellow-related protein
Phlebotomus perniciosus
Phlebotomus orientalis
Salivary protein
Microscale thermophoresis
Biogenic amine

ABSTRACT

The amine-binding properties of sand fly salivary yellow-related proteins (YRPs) were described only in *Lutzomyia longipalpis* sand flies. Here, we experimentally confirmed the kratagonist function of YRPs in the genus *Phlebotomus*. We utilized microscale thermophoresis technique to determine the amine-binding properties of YRPs in saliva of *Phlebotomus perniciosus* and *P. orientalis*, the Old-World vectors of visceral leishmaniases causative agents. Expressed and purified YRPs from three different sand fly species were tested for their interactions with various biogenic amines, including serotonin, histamine and catecholamines. Using the L. *longipalpis* YRP LJM11 as a control, we have demonstrated the comparability of the microscale thermophoresis method with conventional isothermal titration calorimetry described previously. By homology *in silico* modeling, we predicted the surface charge and both amino acids and hydrogen bonds of the amine-binding motifs to influence the binding affinities between closely related YRPs. All YRPs tested bound at least two biogenic amines, while the affinities differ both among and within species. Low affinity was observed for histamine. The salivary recombinant proteins rSP03B (*P. perniciosus*) and rPorASP4 (*P. orientalis*) showed high-affinity binding of serotonin, suggesting their capability to facilitate inhibition of the blood vessel contraction and platelet aggregation.

1. Introduction

Phlebotomus perniciosus and *P. orientalis* are closely related sand fly species (Diptera: Phlebotominae) belonging to the subgenus *Larroussius*. *P. perniciosus* is distributed through the western and central parts of Mediterranean region and it serves as an important vector of *Leishmania infantum,* a causative agent of visceral leishmaniases in Southern Europe and Northern Africa, while *P. orientalis* is a proven vector of *Leishmania donovani* in Sudan, Ethiopia and Kenya (Dvorak et al., 2018). The number of human cases of visceral leishmaniasis were estimated to annually reach up to 20,000 and 56,700, in Mediterranean and East African regions, respectively (Alvar et al., 2012).

To facilitate successful blood feeding, sand fly female injects into the host skin saliva containing a vast variety of pharmacologically active compounds that interact with the host haemostatic processes (Lestinova et al., 2017). To ease the spread of these biomolecules, sand fly saliva contains hyaluronidase, which enzymatic activity facilitates the enlargement of the feeding site by degrading the extracellular matrix (Volfova et al., 2008; Volfova and Volf, 2018). To stop the blood coagulation, sand flies employ anticoagulants which affect the components of coagulation cascade (Chagas et al., 2014; Collin et al., 2012) or inhibit the activators of coagulation (Alvarenga et al., 2013). Some sand fly saliva components such as maxadilan (Lerner and Shoemaker, 1992) and adenosine (Ribeiro et al., 1999) act directly as vasodilatators, while other proteins, such as salivary apyrase prevent the ATP-induced aggregation of platelets (reviewed in Lestinova et al., 2017).

Host haemostatic responses to insect bites are triggered also by biogenic amines such as serotonin, histamine or catecholamines. Serotonin is released by platelets and initiates vasoconstriction resulting in limitation of the flow of blood to the insects mouthparts

Abbreviations: YRP, yellow-related protein; MST, microscale thermophoresis; ITC, isothermal titration calorimetry; HEK293S, human embryonic kidney 293S; Kd, dissociation constant

* Corresponding author. Department of Parasitology, Faculty of Science, Charles University, Vinicna 7, Prague, 12843, Czech Republic.
E-mail address: sumovap@natur.cuni.cz (P. Sumova).

https://doi.org/10.1016/j.ibmb.2019.103245
Received 12 August 2019; Received in revised form 30 September 2019; Accepted 1 October 2019
Available online 08 October 2019

(Ribeiro, 1995). Histamine is secreted upon the tissue damage from basophiles and mast cells granules and influences the hydrostatic pressure of capillaries and their permeability for plasma containing immune cells and other factors (Paesen et al., 1999; Ribeiro and Francischetti, 2003). Both serotonin and histamine have also roles in inducing itch and pain response to the insect bite (Julius and Basbaum, 2001; Yosipovitch et al., 2018). Other biogenic amines playing roles in host haemostatic responses belong to the catecholamine family. Norepinephrine stimulates vasoconstriction via adrenergic receptors in the vasculature (Calvo et al., 2009; Xanthos et al., 2008). When released by the local nerves in response to bleeding, epinephrine also initiates constriction of blood vessels and together with serotonin it potentiates platelet aggregation (Andersen et al., 2003; Francischetti, 2010).

Bloodsucking insects prevent haemostatic responses through binding biogenic amines in the pocket of hollow barrel structure forming the amine-binding proteins belonging into three different protein families (reviewed in Lestinova et al., 2017). Lipocalins serve this function in ticks and triatomine bugs (Andersen et al., 2003; Mans and Ribeiro, 2008; Sangamnatdej et al., 2002; Xu et al., 2013), while D7-related proteins are known kratagonists (= abundant proteins that arrest or seize their bioactive agonists; Ribeiro and Arca, 2009) in mosquitoes (Calvo et al., 2006; Jablonka et al., 2019; Mans et al., 2007). The amine-binding potential of sand fly salivary yellow-related proteins (YRPs) was firstly hypothesized by Charlab et al. (1999). In 2011, the crystal structure and antihaemostatic properties of YRPs of the New-World sand fly *Lutzomyia longipalpis* were revealed. All three L. *longipalpis* YRPs were shown to bind with different affinities serotonin, histamine and catecholamines - epinephrine, norepinephrine, dopamine and octopamine (Xu et al., 2011). Although predicted, the binding of biogenic amines was not yet experimentally demonstrated for YRPs of sand flies from the genus *Phlebotomus*.

To measure the amine-binding interactions of YRPs, several methods can be employed. So far, the isothermal titration calorimetry (ITC) was the method of choice for the characterization of salivary amine-binding proteins of blood-sucking arthropods (Andersen et al., 2003; Calvo et al., 2009, 2006; Jablonka et al., 2019; Ma et al., 2012; Xu et al., 2013, 2011). In sand flies, this method was also utilized to characterize the mechanism of coagulation pathway inhibition in anticoagulants (Alvarenga et al., 2013; Collin et al., 2012). Microscale thermophoresis (MST) was demonstrated as a method comparable with ITC, requiring less sample volume and time (Scheuermann et al., 2016; Seidel et al., 2013; Wienken et al., 2010) but has never been used to characterize binding properties of proteins from blood sucking arthropods.

Here, we have expressed recombinant YRPs from two closely related *Phlebotomus* species, *P. orientalis* (rPorASP4 and rPorASP2) and *P. perniciosus* (rSP03 and rSP03B), and experimentally tested their ability to bind host biogenic amines through MST. To validate the accuracy of our chosen method, we have also expressed and measured binding affinities of *L. longipalpis* YRP LJM11, which ability to bind amines was previously determined using ITC (Xu et al., 2011). We have utilized the 3D models of YRPs to estimate the effect of the amino acid composition of the amine-binding site and of the surface electrostatic potential on the differences in YRPs binding affinities to different biogenic amines.

2. Methods

2.1. Expression of recombinant yellow-related proteins

For binding experiments five salivary YRPs were expressed in human cell line (Table 1). For *P. perniciosus* YRPs, the gene construct was prepared by isolating the total RNA from one day old *P. perniciosus* females by the High Pure RNA Tissue Kit (Roche), after which it was transcribed using anchored-oligo $(dT)_{18}$ primers into the cDNA by Transcriptor First Strand cDNA Synthesis Kit (Roche) following the manufacturer's protocol. The cDNA fragments were amplified by PCR and subcloned into the pTW5sec expression plasmid, a derivative of pTT5 (Blaha et al., 2015; Durocher et al., 2002). Proteins expressed using this plasmid contain additional ITG- and -GTHHHHHHHHG sequences at their N- and C-termini, respectively.

The rSP03B protein was transiently expressed in human embryonic kidney 293S (HEK293S) GnTI$^-$ cell line (ATCC CRL-3022), as previously described in Bláha et al. (2015). Briefly, suspension adapted cells were grown in EX-CELL293 medium supplemented with 4 mM L-glutamine (Sigma) in square-shaped glass bottles at 37 °C and 5% CO_2 in a humidified incubator and shaken at 135 rpm. For transient transfection, the cell culture was transferred into EX-CELL293 medium at 20×10^6 cells/ml cell density. The expression plasmid (diluted in PBS; 1 μg of DNA per 1×10^6 cells) and 25 kDa linear polyethylenimine (in a 1:4 w/w ratio to total amount of DNA) were added directly into the high-density cell culture. After 4 h of incubation, the culture was diluted with EX-CELL293 medium to 2×10^6 cells/ml.

Due to low protein yields, expression cassette of rSP03 was subcloned into vector permitting generation of stably transfected HEK293S GnTI$^-$ cell line using piggyBac system (Li et al., 2013). After selection, pools of stably transfected cells were expanded, and protein expression was induced by doxycycline (1 mg/ml) when cell density reached 3×10^6 cells/ml.

Culture medium was harvested five to seven days post-transfection (rSP03B) or induction (rSP03) by centrifugation (10,000 × *g*, 30 min) and filtered thereafter (0.22 μm Steritop filter; Millipore, USA). Before purification, the harvested medium was diluted with an equal volume of buffer (50 mM Na_2HPO_4, 300 mM NaCl, 10 mM NaN_3, pH 7.5). Histidine-tagged proteins were then purified by IMAC chromatography using HiTrap Talon Crude columns (GE Healthcare) by isocratic (rSP03B) or gradient elution (rSP03). Affinity chromatography was followed by size exclusion chromatography using Superdex 200 Increase 10/300 GL column (GE Healthcare).

Recombinant YRPs derived from *P. orientalis* and *L. longipalpis* were produced and purified as described elsewhere (Gomes et al., 2012; Sumova et al., 2018). Briefly, the synthetic DNA fragments (GeneArt Strings, ThermoFisher Scientific) coding recombinant proteins including histidine tag at the C-terminus were cloned into VR2001-TOPO vector (Oliveira et al., 2006). Plasmids were sent to Leidos, NCI, Protein

Table 1
Recombinant salivary yellow-related proteins.

Name	Species	MW (kDa)	ε ($M^{-1}cm^{-1}$)	GenBank ACCN	Parallel codes
rSP03	*P. perniciosus*	43.20	51,590	ABA43049	PpeSP03[1], Pper1[2]
rSP03B	*P. perniciosus*	44.26	51,590	ABA43050	PpeSP03B[1], Pper2[2]
rPorASP2	*P. orientalis*	42.96	53,080	AGT96427	Pori1[2], mYEL2[3]
rPorASP4	*P. orientalis*	43.74	53,080	AGT96428	Pori2[2], mYEL1[3], PorSP24[4]
LJM11	*L. longipalpis*	44.67	65,000	AAS05318	3Q6K Llon1[2]

List of recombinant YRPs based on the salivary proteins of *P. perniciosus*, *P. orientalis* and *L. longipalpis*. Designation, species, molecular weight (MW), extinction coefficient (ε), GenBank accession numbers and the codes of parallel YRPs are indicated. [1] retrieved from Anderson et al. (2006); [2] Sima et al. (2016b); [3] Sumova et al. (2018); [4] Sima et al. (2016a).

Expression Laboratory (Frederick, MD) for transient transfection and expression. Transfected FreeStyle HEK293 C18 (ATCC CRL-10852) cell cultures were harvested after 72 h. Recombinant proteins were purified in one step in a HPLC system (Bio-Rad) using the HiTrap Chelating HP columns (GE Healthcare) by gradient elution with imidazole.

2.2. Quality check of recombinant proteins

All recombinant YRPs were purified and subsequently stored in phosphate-buffered saline (PBS; pH 7.5). Protein concentrations were measured using a NanoDrop ND-1000 spectrophotometer (ThermoFisher Scientific) at 280 nm and calculated using the theoretical molar extinction coefficients and molecular weights of the proteins (Table 1).

Oligomeric state of all recombinant YRPs was analyzed in analytical ultracentrifuge ProteomeLab XL-I equipped with an An-50 Ti rotor (Beckman Coulter, USA) using the sedimentation velocity experiment. Samples of proteins in PBS buffer were spun at 48,000 rpm at 20 °C, and 100 scans with 0.003 cm spatial resolution were recorded at 280 nm in 5-min steps using absorbance optics. Buffer density and protein partial specific volumes were estimated in SEDNTERP (www.jphilo.mailway.com). Data were analyzed with Sedfit (Schuck, 2000) using a c(s) continuous size distribution model, figure illustrating AUC data was prepared in GUSSI (Brautigam, 2015).

To check the quality of expressed proteins, 1 µg of each eligible protein fractions acquired from chromatography was electrophoretically separated on 12% polyacrylamide gel under non-reducing conditions using a Mini-protean apparatus (Bio-Rad). One gel with separated proteins was silver stained. Separated protein bands from parallel gel were transferred onto a nitrocellulose membrane using the iBLOT system (Invitrogen) and blocked in 5% non-fat milk diluted in a Tris-buffered saline with 0.05% Tween 20 (TBS-Tw) overnight at 4 °C. Subsequently, the membrane was incubated for 1 h with a monoclonal anti-polyhistidine-peroxidase antibody (Sigma Aldrich) diluted 1:1000 in TBS-Tw. After the washing step with TBS-Tw, the chromogenic reaction was developed using a substrate solution containing diaminobenzidine and H_2O_2. Identity and high purity of the proteins was further verified by mass spectrometry.

2.3. Mass spectrometry

Mass spectrometry was used to confirm the high purity of expressed proteins, to estimate the proportion of *P. orientalis* and *P. perniciosus* YRPs in the total amount of salivary glands proteins and to determine the ratio of the two YRPs in both species. The analyses were performed in OMICS Proteomics laboratory Biocev, Czech Republic. For the analysis, salivary glands were dissected from 5 to 7 day old sand fly females into aliquots of 20 glands per 20 µl of 100 mM triethylammonium bicarbonate buffer with 2% sodium deoxycholate and boiled at 95 °C for 5 min. Protein samples (20 µg of each YRP per sample) were mixed with 4 vol of cold ice acetone and kept for 30 min at −20 °C, then centrifuged for 15 min at 16,000 × *g* at 4 °C. Supernatants were discarded and pellets were resuspended in the same buffer as for salivary glands.

Subsequently, cysteines were reduced by 5 mM tris(2-carboxyethyl) phosphine (TCEP; 60 min at 60 °C), blocked with 10 mM of methylmethanethiosulfonate and incubated 10 min at RT. Samples were digested with trypsin at 37 °C overnight, after which they were acidified with trifluoroacetic acid up to a final concentration of 1%. Finally, sodium deoxycholate was removed by extraction to ethyl acetate (Masuda et al., 2008) and the peptides were desalted on a Michrom C18 column.

The Nano Reversed phase column (EASY-Spray PepMap C18 column, 50 cm × 75 µm ID, 2 µm particles, 100 Å pore size) was used for the LC/MS analysis. The mobile phase A was composed of 0.1% formic acid, while the mobile phase B was composed of acetonitrile and 0.1% formic acid. Samples were loaded onto the peptide trap column (Acclaim PepMap 300 C18, 5 µm, 300 Å pore size, 300 µm × 5 mm) at a flow rate of 15 µl/min. The loading buffer was composed of water, 2% acetonitrile and 0.1% trifluoroacetic acid. Peptides were eluted with gradient of B from 4% to 35% during 60 min at a flow rate of 300 nl/min. The eluted peptides were converted to gas phase ions using electrospray ionization and subsequently analyzed on a Thermo Orbitrap Fusion (Q-OT-qIT, Thermo). Survey scans of peptide precursors from 350 to 1400 m/z were performed at 120K resolution (at 200 m/z) with a 5×10^5 ion count target. Tandem MS was performed by isolation at 1.5 Th with the quadrupole, higher energy collisional dissociation fragmentation with normalized collision energy of 30, and rapid scan MS analysis in the ion trap. The MS 2 ion count target was set to 10^4 and the maximum injection time was 35 ms. Only the precursors with a charge state of 2–6 were sampled for MS 2. The dynamic exclusion duration was set to 45 s with a 10 ppm tolerance around the selected precursor and its isotopes. Monoisotopic precursor selection was turned on. The instrument was run in top speed mode with 2 s cycles (Hebert et al., 2014).

All data were analyzed and quantified with the MaxQuant software (version 1.5.3.8) (Cox et al., 2014). The false discovery rate was set to 1% and we specified a minimum length of seven amino acids. The Andromeda search engine was used for the MS/MS spectra search against the database obtained from the available sand fly transcriptomes (for samples from salivary glands), or from the Human database (downloaded from Uniprot on September 2017, containing 20,142 entries). Enzyme specificity was set as C-terminal to arginine and lysine, also allowing cleavage at proline bonds and a maximum of two missed cleavages. Dithiomethylation of cysteine was selected as the fixed modification and N-terminal protein acetylation and methionine oxidation as variable modifications. Finally, data analysis was performed using Perseus 1.5.2.4 software (Tyanova et al., 2016). Proteins purities/ratios were calculated as percentages of intensities of particular proteins from summed intensities of all identified proteins.

2.4. Microscale thermophoresis

Microscale thermophoresis (MST) was used to measure the binding between recombinant YRPs and their potential ligands, the biogenic amines. This approach is based on the measurement of the ligand binding induced change in directed movement of molecules along a temperature gradient. The change in movement is caused by differences in size, charge, or solvation energy of the studied protein itself versus in complex with the ligand. This change is measured by monitoring the fluorescence of label attached to the protein (Baaske et al., 2010).

The highly pure recombinant YRPs were fluorescently labeled by Monolith Protein Labeling Kit RED-NHS (Nanotemper) according to manufacturer instructions. Fluorescent YRPs were then diluted to 6 nM concentration (corresponding to 260 ng/ml) in the MST buffer (50 mM Tris-HCl, pH 7.4; 150 mM NaCl; 10 mM $MgCl_2$; 0.05% Tween-20) and centrifuged for 10 min at 15,000 × *g* at 4 °C to get rid of protein aggregates. The biogenic amines serotonin, histamine, dopamine, octopamine, norepinephrine and epinephrine (Sigma) were dissolved in MST buffer. For each tested recombinant YRP, a titration series with constant concentration of fluorescently labeled YRP and equal amount of two-fold dilution series of a single unlabeled ligand was prepared in the MST buffer. Binding experiments were performed on a Monolith NT.115PicoRed (Nanotemper). Samples were loaded into the Monolith NT.115 Premium Capillaries (Nanotemper) and ran with 40% MST power and 10–20% LED power based on the fluorescence signal of each protein. The Kd (dissociation constant) model binding curves expressing the dependence of normalized fluorescence on the ligand concentration were fitted to the average of three independent repetition of each experiment. The Kd values, confidence intervals, amplitudes and the signal to noise levels were calculated using the NanoTemper analytical software package. The amplitude of the binding interaction expressed the difference in normalized fluorescence values between the

bound and unbound state (signal). The noise level was defined as the average standard deviation of all data points compared to the Kd model curve. The signal-to-noise ratio was used to assess the quality of the binding outcome, with a ratio higher than 5 being desirable and ratio higher than 12 reflecting an excellent assay according to manufacturer's manual. For the purposes of this study we have defined the strength of the binding interaction as high when the measured Kd was lower than 10 nM, medium when Kd was in range of 10–1000 nM, low for Kd in range of 1–10 μM and poor for Kd higher than 10 μM.

2.5. 3D models

The YRPs were modeled as described in Sima et al. (2016b). Models were based on the crystal structure of LJM11, the only available sand fly YRP in Protein Data Bank (3Q6K; Xu et al., 2011). Models and their amine-binding site were displayed and analyzed in PyMOL (The PyMOL Molecular Graphics System, Version 1.5, Schrödinger, LLC.). Electrostatic surface potentials were calculated using the APBS Tools 2 plug-in (Baker et al., 2001) in PyMOL.

3. Results and discussion

Yellow-related proteins (YRPs) are characterized by the presence of major royal jelly protein domain (Schmitzova et al., 1998) and their name is derived from the role of “yellow” protein in cuticle pigmentation in *Drosophila* (Geyer et al., 1986). So far, YRPs were found only in sand fly salivary proteomes. Presence of YRP in the midgut was once reported (Volf et al., 2002), but it seems that the protein was swallowed there with saliva. YRPs are abundant in saliva of all sand fly species studied up-to-date (Abdeladhim et al., 2016, 2012; Anderson et al., 2006; Coutinho-Abreu and Valenzuela, 2018; de Moura et al., 2013; Hostomska et al., 2009; Kato et al., 2013, 2006; Oliveira et al., 2006; Rohousova et al., 2012; Valenzuela et al., 2004; Vlkova et al., 2014). In each sand fly species, 1–5 YRPs of distinct sequences with molecular weight of 41–45 kDa were described. In sand fly saliva, YRPs are predicted to act as high affinity binders of host's pro-haemostatic and pro-inflammatory biogenic amines, such as serotonin, histamine and catecholamines but previously this binding was experimentally verified only for YRPs from New-World sand fly species *L. longipalpis* (Xu et al., 2011). Here, we have tested the amine-binding capability of YRPs in the two species of the Old-World genus *Phlebotomus* and validated microscale thermophoresis (MST) as an accurate method to determine the binding affinities of biogenic amines to YRPs.

3.1. YRPs in salivary glands

Among proteins determined by mass spectrometry in the *P. perniciosus* and *P. orientalis* salivary gland homogenates, YRPs constitute a high proportion; 40% and 35.4%, respectively. These portions correspond to approximately 160 ng and 100 ng of YRPs per a pair of salivary glands of *P. perniciosus* and *P. orientalis*, respectively (Sumova et al., 2018; Velez et al., 2018). The two YRPs in each species tested were present in ratio 2.67 for rSP03B/rSP03 and 2.52 for rPorASP4/rPorASP2 making the closely related proteins rSP03B and rPorASP4 considerably more abundant than the other two YRPs (S1 Table;Sumova, 2019 [dataset]). The potential of both rSP03B and rPorASP4 to sequester biogenic amines is therefore enhanced by the higher quantities of these proteins salivated into the host skin.

To antagonize host haemostasis through sequestering the biogenic amines at the biting site, the amine-binding proteins should presumably achieve the concentrations corresponding to 0.2–2 μM, which in mosquitoes correspond to 0.03–0.3 μg of amine-binding D7 proteins (Calvo et al., 2006). In mosquitoes, both the blood meal (2.4–3.3 μl) and the salivary proteins amount per a pair of glands (1.4–4 μg) are in average 5 times larger than in studied sand flies (0.6 μl and 0.3–0.4 μg, respectively) (Jeffery, 1956; Nascimento et al., 2000; Pruzinova et al., 2015). Therefore, after recalculation according to YRPs molecular weight, we can consider 17–174 ng of YRPs necessary for physiological relevance. As both mosquitoes and sand flies discharge during blood feeding approximately half of the salivary proteins content (Marinotti et al., 1990; Ribeiro et al., 1989), we can consider the measured amount of YRPs sufficient to scavenge local biogenic amines. YRPs are therefore present in salivary glands in physiologically significant quantities to act as kratagonists.

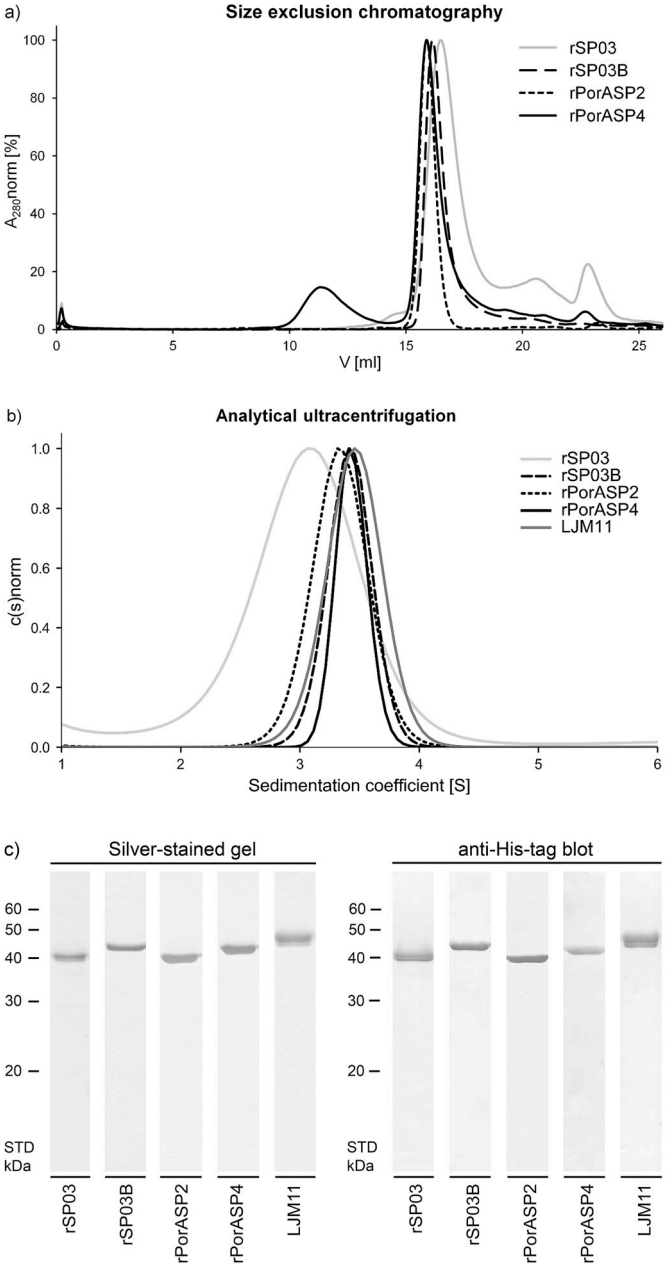

Fig. 1. Purification and quality control of recombinant proteins. a) Representative results of size exclusion chromatography (Superdex 200 Increase 10/300 GL, GE Healthcare); peaks for each protein are shown with distinct type of line (see legend on the right). b) Recombinant YRPs were analyzed in analytical ultracentrifuge by sedimentation velocity experiment and an overlay of normalized size distributions for individual proteins is shown. c) Recombinant YRPs were run by SDS-PAGE under non-reducing conditions. Silver-stained gel is shown on the left. Western blot analysis was performed with anti-polyHistidine-peroxidase antibody. Molecular weights (kDa) of standard (STD; BenchMark Protein Ladder, ThermoFisher Scientific) are indicated.

3.2. Recombinant yellow-related proteins

All YRPs with a histidine-tag were expressed in a HEK293 cell line and purified by chromatography; the representative results for *P. perniciosus* and *P. orientalis* YRPs are shown in Fig. 1a. All recombinant proteins were analyzed in an analytical ultracentrifuge by performing sedimentation velocity experiment. The resulting size distributions of sedimenting species are shown in Fig. 1b. Apart from rSP03, all other proteins have standard $s_{20,w}$ sedimentation coefficient of 3.5–3.6 S, corresponding well to anticipated 43–45 kDa monomeric proteins. Protein rSP03 sedimented slower with $s_{20,w}$ of 3.2 S, suggesting slightly different shape of the particle when compared to other measured YRPs. The purity of proteins was verified by SDS-PAGE and Western blot analysis with an anti-histidine-tag antibody. Both the silver stained gel and the Western blot assay showed only one major band of expected molecular weight for all YRP tested (Fig. 1c). The purity of all YRPs was verified by high-resolution mass spectrometry and reached 91% in average. The major contaminants were identified as keratins, whose presence in samples resulted from protein handling and do not interfere with YRPs performance.

The amino acid similarities between studied recombinant YRPs are summarized in Table 2. The highest similarity was found between YRPs originating from different *Phlebotomus* species, reaching 86% amino acid sequence identity for rSP03 and rPorASP2, and 85% for rSP03B and rPorASP4. High degree of identity found between rSP03/rPorASP2 and rSP03B/rPorASP4 is in accordance with their position on phylogenetic tree, where they form the same clusters together with YRPs from related *Larroussius* species *P. tobbi* (Abdeladhim et al., 2016; Coutinho-Abreu and Valenzuela, 2018; Sima et al., 2016b). As expected for a species from different genera, *L. longipalpis* LJM11 share only 51–55.6% identity with *Phlebotomus* YRPs.

3.3. Ligand binding analysis using microscale thermophoresis

Microscale thermophoresis was used to determine whether the expressed recombinant YRPs bind different biogenic amines. Binding curves modeled for each protein with binding amines are shown in Fig. 2. Dissociation constants (Kd) of the interaction of each YRP with all ligands derived from these data are summarized in Table 3. The calculated amplitudes and signal to noise ratios were high enough to confirm the significances of the binding curves for all measured binding interactions.

Protein rSP03 acted as a medium affinity binder of norepinephrine, low affinity binder of octopamine and a poor affinity binder of histamine, epinephrine and serotonin. The binding curve for dopamine was affected by the ligand induced change in fluorescence which precluded plotting it into graph. We have estimated the Kd for dopamine to be higher than 20 μM thus making it a poor affinity ligand. The second *P. perniciosus* YRP, protein rSP03B, had affinity for two ligands only. It served as a high affinity binder of serotonin and it also interacted poorly with histamine. Protein rPorASP2 bound with high affinity octopamine, with medium affinity serotonin and dopamine and it poorly bound histamine. rPorASP2 had no measurable affinity for catecholamines epinephrine and norepinephrine. Protein rPorASP4 interacted with different strength with all ligands. It displayed a high affinity for serotonin and dopamine, medium affinity to norepinephrine, octopamine and epinephrine, and it interacted with low affinity with histamine. The binding interactions of LJM11 were similar to those measured for rPorASP4; the only variation was detected in the lower affinities of LJM11 for epinephrine and histamine. The binding affinities of LJM11 measured by MST correspond well with the ones measured previously by the ITC technique (Table 3, square brackets; Xu et al., 2011). We have therefore shown that for this type of study the results obtained either by ITC or MST are comparable.

Although the binding of biogenic amines to YRPs varied both among and within sand fly species, we can draw the following conclusions: In both *P. orientalis* and *P. perniciosus*, at least one YRP was shown to bind with high affinity serotonin (Kd $<$ 10 nM) and with medium affinity norepinephrine (Kd = 10–1000 nM), suggesting that both sand fly species effectively sequester these compounds during feeding. This YRPs capability might inhibit the blood vessels contraction and impede platelet activity by increasing the agonist threshold concentration for the platelet aggregation (Andersen et al., 2003; Calvo et al., 2006). This effect can be further emphasized by the high abundance of both high affinity binders of serotonin (rSP03B and rPorASP4) in sand fly saliva. On the contrary, all tested proteins bound histamine with affinity lower than 1 μM which was indicated as insufficient to prevent interaction of histamine with its physiological receptors (Mans et al., 2008; Xu et al., 2011). To our knowledge, there are recently no other histamine-binding candidates in sand flies. Sand flies D7-related proteins, whose counterparts serve this function in mosquitoes, were recently shown not to contain the essential amine-binding pocket (Jablonka et al., 2019).

The binding affinities for epinephrine, dopamine and octopamine varied among the individual YRPs. When comparing the two *Phlebotomus* species, the binding affinities were in *P. perniciosus* much lower for all these potential ligands. Observed species-specific differences in amine-binding properties could be hardly explained by different feeding behavior as both *Phlebotomus* species studied share similar host preferences. Despite the tight binding of dopamine and octopamine to *P. orientalis* YRPs, these ligands are improbable physiological targets for the salivary YRPs, as they do not play a major role in haemostasis or inflammation (Xu et al., 2011). Therefore, the interspecific difference in binding of these catecholamines is not supposed to have an application in physiological conditions. We may hypothesize that the only physiological activity of sand flies YRPs is to bind serotonin, while binding the other amines might be artifact of their similar structure. Therefore both sand fly species have one functional YRP which binds serotonin with very high affinity.

Table 2
Recombinant YRPs amino acid sequence identity.

	LJM11	rSP03	rPorASP2	rPorASP4	rSP03B
LJM11	——	51.06	53.32	55.56	51.45
rSP03	51.06	——	85.98	75.65	68.49
rPorASP2	53.32	85.98	——	76.96	68.25
rPorASP4	55.56	75.65	76.96	——	84.82
rSP03B	51.45	68.49	68.25	84.82	——

Percent identity matrix of recombinant YRPs created in Clustal Omega (Sievers et al., 2011).

3.4. Amine-binding site

The YRPs amine-binding site was formerly determined from LJM11 crystals with added serotonin (Xu et al., 2011). The site was shown to be composed by 11 amino acids from which eight bound biogenic amines through van der Waals forces and hydrophobic interactions. Five of these amino acids are conserved in all YRPs modeled up to date. Three extra amino acids (Thr327, Asn 342 and Phe 344) of the LJM11 binding motif were able to bind serotonin not only by above mentioned non-covalent intermolecular interactions, but also by hydrogen bonds (Fig. 3), which are predicted to play major role in the binding event (Sima et al., 2016b; Xu et al., 2011).

We have modeled the major amino acids together with their hydrogen bond interactions in the amine-binding site of all YRPs tested (Fig. 3). In *P. orientalis* rPorASP4, the binding motif differed only in one amino acid (position 344; Gln instead of Phe) from *L. longipalpis* LJM11, though the amino acid sequence identity of these two proteins is only 55.6%. This non-conservative substitution should not alter the potential hydrogen bond of the carbonyl oxygen; on the contrary it could facilitate the link of additional hydrogen bond to the glutamine side chain

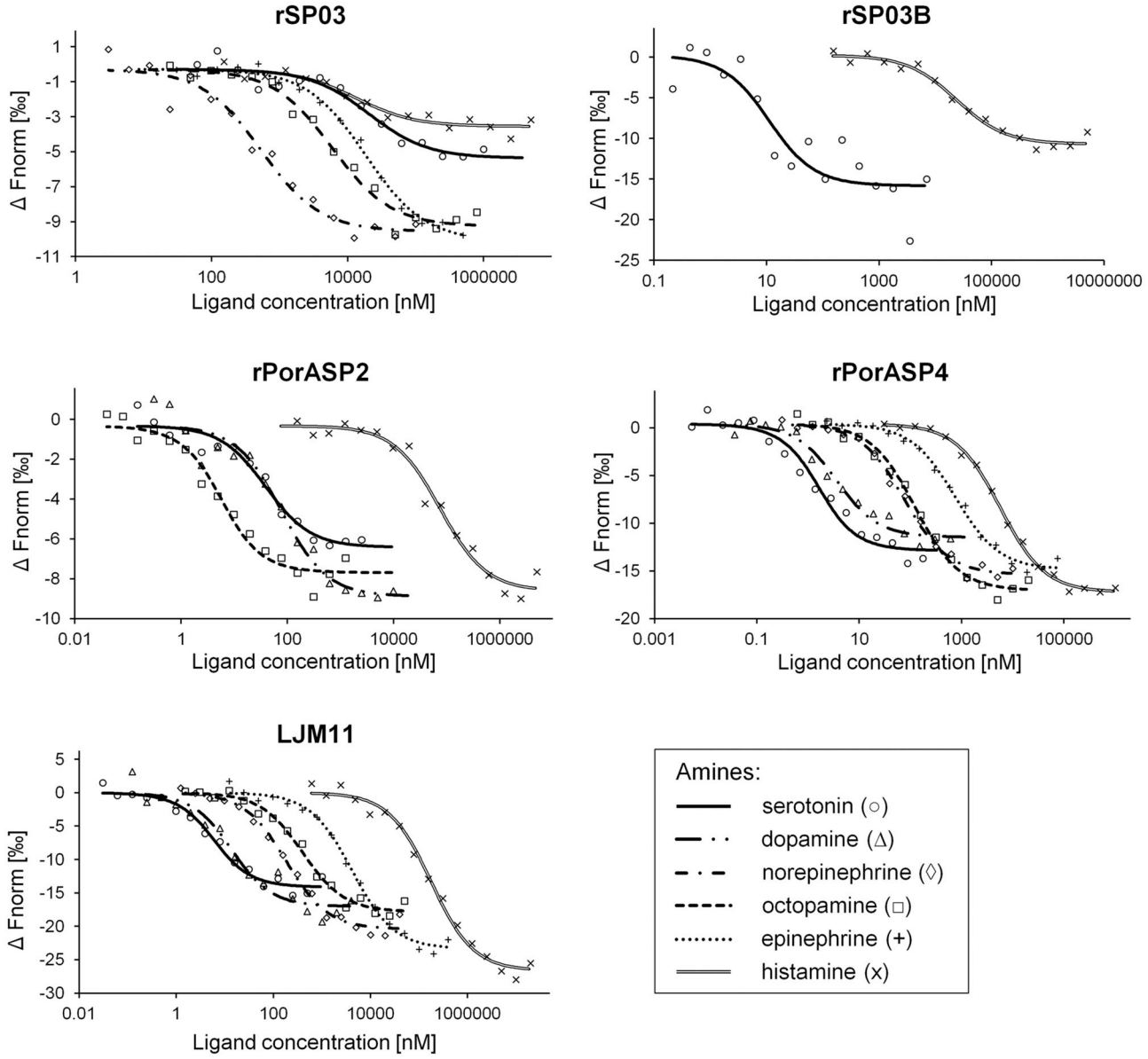

Fig. 2. MST showing binding of biogenic amines to each YRP. Graphs show the MST data fitted with Kd model binding curves for each YRP and all the biogenic amines it bound. For the amines for which no binding was detected, no graphical visualization is shown. Each curve and data point represents an average of three independent experiments. Curves for each amine are shown with distinct type of line and data points (see legend in frame).

and therefore tightening the interaction with serotonin (Sima et al., 2016b). This assumption was emphasized by the measured high affinity interaction of rPorASP4 with serotonin, which achieved the lowest Kd of all proteins tested.

The highly related proteins rSP03 and rPorASP2 (86% identity) shared the same amine-binding motif differing from LJM11 in one non-conservative substitution at position 344 (His instead of Phe), which should not affect the distance of putative hydrogen bond; and one conservative substitution within the other amino acids of the binding motif.

Protein rSP03B varied in all 3 amino acids playing major role in the ligand binding in addition to conservative substitutions in other two amino acids of the amine-binding motif. Conservative substitution at the position 327 (Ser instead of Thr) and non-conservative substitution at the position 344 (His instead of Phe) probably did not affect the putative hydrogen bonds to serotonin. On the contrary, the conservative substitution at the position 342 (Thr instead of Asn) probably resulted in the switch of two potential hydrogen bonds to only one. Previously described site-directed mutagenesis of an asparagine to alanine at the position 342 resulted for LJM11 in elimination of both potential hydrogen bonds. This mutation led to the complete loss of binding to norepinephrine and epinephrine and to the large reduction of the affinity for serotonin and dopamine (histamine and octopamine were excluded from the analysis) (Xu et al., 2011). This finding is in accordance with the measured absence of binding of all catecholamines by rSP03B. The fact that SP03B was shown to bind serotonin with high affinity can be explained by the protein retaining one hydrogen bond at the side chain of threonine which is larger and therefore closer to the

Table 3
Amine-binding properties of recombinant YRPs.

YRP	Ligand	Kd (nM)	Kd CI	Amplitude	Signal to Noise
rSP03	Serotonin	20,558	± 7062	5.1	10.0
	Dopamine	> 20,000	NA	NA	NA
	Norepinephrine	534	± 131	9.3	13.1
	Epinephrine	18,418	± 1920	9.8	33.6
	Octopamine	5935	± 1160	9.0	17.1
	Histamine	13,138	± 4431	3.3	9.6
rSP03B	Serotonin	9.6	± 6.2	16.1	5.4
	Dopamine	NB	± NA	NA	NA
	Norepinephrine	NB	± NA	NA	NA
	Epinephrine	NB	± NA	NA	NA
	Octopamine	NB	± NA	NA	NA
	Histamine	23,708	± 4602	10.9	16.5
rPorASP2	Serotonin	37.5	± 10	6.1	13.0
	Dopamine	76.4	± 20.8	8.6	12.0
	Norepinephrine	NB	± NA	NA	NA
	Epinephrine	NB	± NA	NA	NA
	Octopamine	4.2	± 1.2	7.4	13.2
	Histamine	75,107	± 20,800	8.3	16.2
rPorASP4	Serotonin	1.1	± 0.3	13.3	13.2
	Dopamine	3.2	± 0.7	11.9	15.7
	Norepinephrine	74.8	± 8.4	15.8	28.9
	Epinephrine	745	± 79.2	15.2	30.4
	Octopamine	122	± 16.2	17.5	24.3
	Histamine	5753	± 378	17.6	48.7
LJM11	Serotonin	4.5 [4.3]	± 1.1	14.1	15.5
	Dopamine	12.4 [12]	± 4.0	17.0	10.5
	Norepinephrine	182 [63]	± 24.6	20.4	23.8
	Epinephrine	4212 [454]	± 465	23.4	29.3
	Octopamine	396 [217]	± 61.9	17.8	20.6
	Histamine	178,801 [> 1000]	± 23,426	26.6	24.6

Dissociation constants (Kd; nM), Kd confidence intervals (CI), amplitudes and the signal to noise ratios for rSP03, rSP03B, rPorASP2, rPorASP4 and LJM11. The dissociation constants measured previously for protein LJM11 by ITC (Xu et al., 2011) are presented in square brackets. NB – no measurable binding interaction, NA – not applicable.

serotonin than in the case of alanine (Fig. 3.). The expected decrease of affinity to catecholamines could have been further enhanced by the substitutions in other amino acids possibly influencing the interaction of rSP03B with the secondary and phenolic hydroxyls, which were previously shown to have an important role in the binding interactions of mosquitoes amine-binding proteins (Calvo et al., 2009; Mans et al., 2007).

The majority of the measured substitutions in the amine-binding motif had presumably no effect on the putative hydrogen bonds holding the ligand in the binding pocket. We can therefore hypothesize that there are other factors which should be considered when analyzing the differences in the YRPs affinities for different ligands. For instance, the low affinity binding of histamine by all YRPs might be due to the absence of hydrogen bond formation towards hydroxyl groups, which are not present in the structure of this ligand. Even though the ligand-binding sites of insect amine-binding proteins were by crystallography (Calvo et al., 2009; Mans et al., 2007), site-directed mutagenesis (Mans et al., 2007; Xu et al., 2011) or by ligand saturation experiments (Andersen et al., 2003) repeatedly shown to be analogous for different biogenic amines, it is possible that the ligands may in each protein accommodate a slightly different position disabling, reducing or conversely increasing their binding affinity (Calvo et al., 2009; Xu et al., 2013).

3.5. 3D models and electrostatic potential of YRPs

L. longipalpis YRPs share a similar six-bladed β-propeller fold with all sand fly YRPs studied up to date, which were all shown by homology modeling to comprise a ligand-binding site within their barrel structure (Sima et al., 2016b). The electrostatic potential of the *P. perniciosus*, *P. orientalis* and *L. longipalpis* YRPs surface was compared on their 3D models (Fig. 4). The models of both entrance sides of the six-bladed β-propeller structure showed that the cavity of the channel has in all cases negative charge, which enables the binding of positively charged bioamines in all YRPs studied. This is in accordance with the negatively charged amine-binding site of structurally similar D7 proteins in mosquitoes (Calvo et al., 2009).

Closely related proteins rSP03 and rPorASP2 were shown to share the negative electrostatic potential at both channel openings. Other proteins shared predominantly neutral charge at the entrance of the side further from the ligand-binding site. The charge on the side closer to the ligand was found more variable, with the proteins LJM11, rPorASP4 and rSP03B displaying positive, negative and predominantly neutral electrostatic potential, respectively. Proteins rPorASP4 and LJM11, which were shown to have similar binding affinities, had opposite charges at the channel entrance closer to the binding site, but shared the same charges on the other side of the channel (Fig. 4). We can therefore hypothesize that the ligands preferably enter the barrel structure from the side further from the binding pocket. This assumption is in agreement with already described larger size of this entrance in all YRPs, which could facilitate the entry of the ligand (Sima et al., 2016b). If this hypothesis is valid, the surface charge will probably have less pronounced effect on binding interactions than expected.

The observed variance in the binding affinities even of closely related YRPs was shown also in the three *L. longipalpis* YRPs indicating the occurrence of functional divergence in the family (Xu et al., 2011). Divergence in YRPs function might be caused also by other factors apart from the variations in the amine-binding motif and charge. This can be illustrated on proteins rPorASP2 and rSP03, which share the same amine-binding motif and electrostatic potential but differed in binding affinities for all ligands. Interestingly, rSP03 protein showed slightly lower value of sedimentation coefficient than expected according to its molecular weight and also lower than all other analyzed YRPs (Fig. 1b), pointing to more elongated shape or slightly different folding of this protein compared to other tested YRPs, which might be the cause of different binding properties of rSP03. Distinct interactions of rSP03 and rPorASP2 might be also influenced by the absence of N-glycosylation in rPorASP2 (Sima et al., 2016b; Vlkova et al., 2014) presumably affecting the protein folding and subsequently its structure and therefore also binding properties (Katoh and Tiemeyer, 2013). The particular sand fly YRPs were also found versatile in other parameters including the length, minimum radius and hydrophobicity of their channels, which could also affect the binding affinities even of closely related proteins (Sima et al., 2016b).

In conclusion, we have validated MST as a useful tool to study the amine-binding interactions of the sand fly YRPs. We have shown that although the 3D structure of all YRPs is highly conserved, differences in the amino acids of the ligand-binding motif, conformation of the potential ligands and other factors might affect the binding affinities even of closely related proteins. Nevertheless, both *P. orientalis* and *P. perniciosus* express at least one YRP which bound serotonin with high affinity, while none of the proteins was shown to bind histamine with significant affinity. We can therefore propose that both *P. perniciosus* and *P. orientalis* YRPs potentially contribute to counteracting of the platelet aggregation and vasoconstriction.

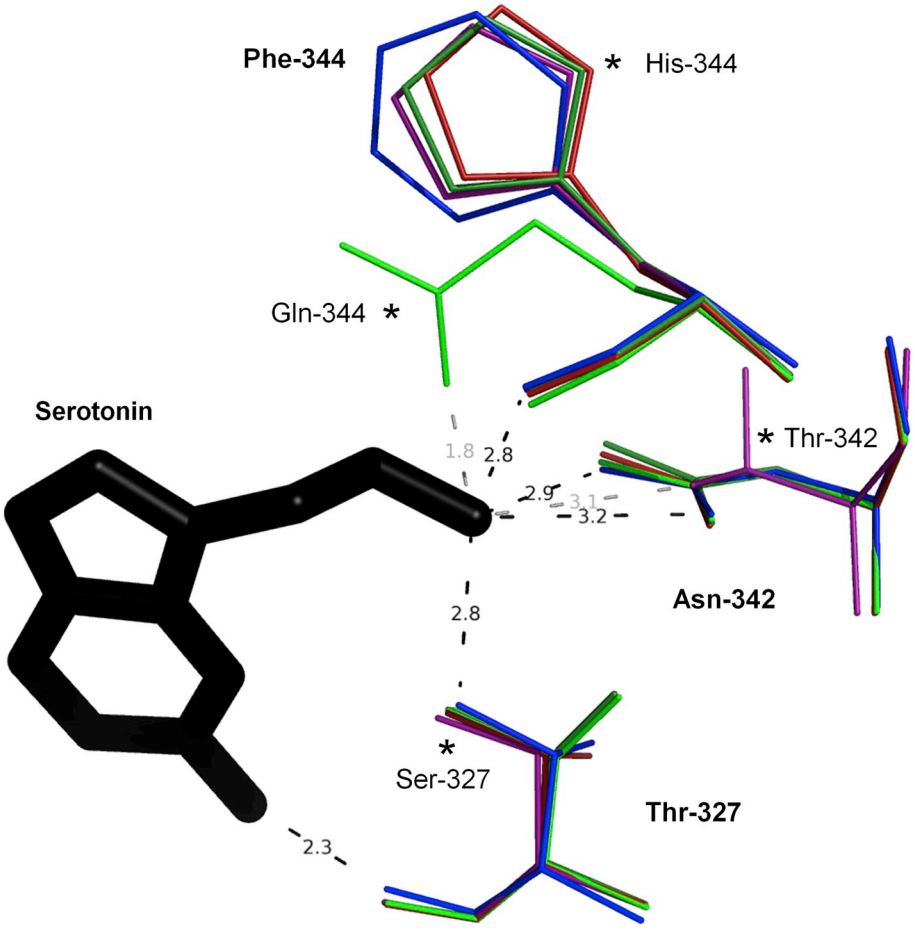

Fig. 3. Amine-binding pocket of YRPs. The model depicts the relevant amino acids of the serotonin binding site for both *P. perniciosus* (rSP03 - red, rSP03B - violet) and *P. orientalis* (rPorASP2 - dark green, rPorASP4 - light green) YRPs and *L. longipalpis* protein LJM11 (blue). Numbering of amino acids was adapted from Xu et al. (2011). Dashed lines represent putative hydrogen bonds which bind serotonin (black) inside the pocket, the numbers mark the actual donor-acceptor distances in Ångströms, in grey are marked the bonds formed by the amino acid substitutions. Asterisks mark the substitutions in amino acids participating in hydrogen bond formation. (For interpretation of the references to colour in this figure legend, the reader is referred to the Web version of this article.)

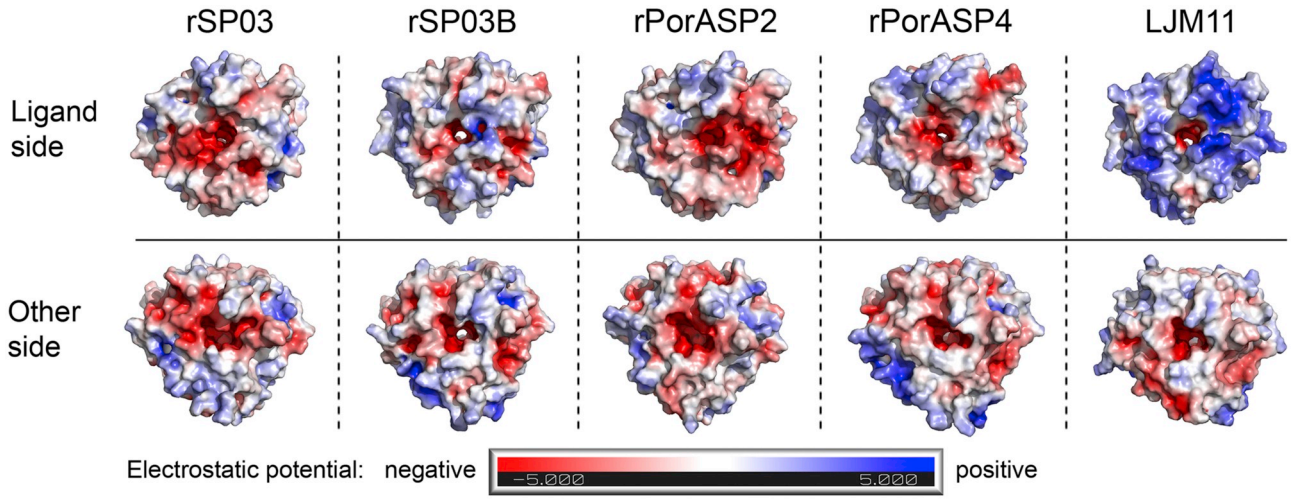

Fig. 4. Electrostatic potential at YRPs channel entrances. Models depict each recombinant YRP from side closer (ligand side) and further (other side) to the ligand-binding site inside the channel. Color and its brightness correspond to the scale of negative (red) to positive (blue) charge. (For interpretation of the references to colour in this figure legend, the reader is referred to the Web version of this article.)

Funding

This work was supported by the Charles University, Czech Republic (GAUK project no. 120516/B-BIO; PS); Czech Science Foundation, Czech Republic (project no. P506 17-10308S; MS, PS, NP, PV); the Ministry of Education, Youth and Sports of the Czech Republic (LTC17065 in frame of the COST Action CA15126); Centre for research of pathogenicity and virulence of parasites (CZ.02.1.01/0.0/0.0/16_019/0000759; PV) and by the project „BIOCEV – Biotechnology and Biomedicine Centre of the Academy of Sciences and Charles University“ (CZ.1.05/1.1.00/02.0109) from the European Regional Development Fund. BK has received financial support from Charles University, Czech

Republic under the SVV260427/2019. This research was supported in part by the Intramural Research Program of the NIH, National Institute of Allergy and Infectious Diseases, United States (FO, JGV). The funders had no role in the study design, data collection and analysis, decision to publish, or preparation of the manuscript.

Acknowledgement

We are grateful to Shannon Townsend and Morgan Karetnick for the help with protein expression in mammalian system. Our thanks are due to Vera Volfova for providing us with the sand fly image. Acknowledgement to Karel Harant and Pavel Talacko from Laboratory of Mass Spectrometry, Biocev, Charles University, Faculty of Science, where proteomic and mass spectrometric analysis had been done. We appreciate Helena Kulikova and Lenka Krejcirikova for excellent technical and administrative support.

References

Abdeladhim, M., Jochim, R.C., Ben Ahmed, M., Zhioua, E., Chelbi, I., Cherni, S., Louzir, H., Ribeiro, J.M.C., Valenzuela, J.G., 2012. Updating the salivary gland transcriptome of *Phlebotomus papatasi* (Tunisian strain): the search for sand fly-secreted immunogenic proteins for humans. PLoS One 7, e47347. https://doi.org/10.1371/journal.pone.0047347.

Abdeladhim, M.V., Coutinho-Abreu, I., Townsend, S., Pasos-Pinto, S., Sanchez, L., Rasouli, M.B., Guimaraes-Costa, A., Aslan, H., Francischetti, I.M.B., Oliveira, F., Becker, I., Kamhawi, S., Ribeiro, J.M.C., Jochim, R.C., Valenzuela, J.G., 2016. Molecular diversity between salivary proteins from New World and Old World sand flies with emphasis on *Bichromomyia olmeca*, the sand fly vector of *Leishmania mexicana* in Mesoamerica. PLoS Neglected Trop. Dis. 10, e0004771. https://doi.org/10.1371/journal.pntd.0004771.

Alvar, J., Velez, I.D., Bern, C., Herrero, M., Desjeux, P., Cano, J., Jannin, J., de Boer, M., 2012. Leishmaniasis worldwide and global estimates of its incidence. PLoS One 7, e35671. https://doi.org/10.1371/journal.pone.0035671.

Alvarenga, P.H., Xu, X., Oliveira, F., Chagas, A.C., Nascimento, C.R., Francischetti, I.M.B., Juliano, M.A., Juliano, L., Scharfstein, J., Valenzuela, J.G., Ribeiro, J.M.C., Andersen, J.F., 2013. Novel family of insect salivary inhibitors blocks contact pathway activation by binding to polyphosphate, heparin, and dextran sulfate. Arterioscler. Thromb. Vasc. Biol. 33, 2759–2770. https://doi.org/10.1161/ATVBAHA.113.302482.

Andersen, J.F., Francischetti, I.M.B., Valenzuela, J.G., Schuck, P., Ribeiro, J.M.C., 2003. Inhibition of hemostasis by a high affinity biogenic amine-binding protein from the saliva of a blood-feeding insect. J. Biol. Chem. 278, 4611–4617. https://doi.org/10.1074/jbc.M211438200.

Anderson, J.M., Oliveira, F., Kamhawi, S., Mans, B.J., Reynoso, D., Seitz, A.E., Lawyer, P., Garfield, M., Pham, M., Valenzuela, J.G., 2006. Comparative salivary gland transcriptomics of sandfly vectors of visceral leishmaniasis. BMC Genomics 7, e52. https://doi.org/10.1186/1471-2164-7-52.

Baaske, P., Wienken, C.J., Reineck, P., Duhr, S., Braun, D., 2010. Optical thermophoresis for quantifying the buffer dependence of aptamer binding. Angew. Chem. Int. Ed. 49, 2238–2241. https://doi.org/10.1002/anie.200903998.

Baker, N.A., Sept, D., Joseph, S., Holst, M.J., McCammon, J.A., 2001. Electrostatics of nanosystems: application to microtubules and the ribosome. Proc. Natl. Acad. Sci. 98, 10037–10041. https://doi.org/10.1073/pnas.181342398.

Blaha, J., Pachl, P., Novak, P., Vanek, O., 2015. Expression and purification of soluble and stable ectodomain of natural killer cell receptor LLT1 through high-density transfection of suspension adapted HEK293S GnTI- cells. Protein Expr. Purif 109, 7–13. https://doi.org/10.1016/j.pep.2015.01.006.

Brautigam, C.A., 2015. Calculations and publication-quality illustrations for analytical ultracentrifugation data. In: Methods in Enzymology. Elsevier Inc., pp. 109–133.

Calvo, E., Mans, B.J., Andersen, J.F., Ribeiro, J.M.C., 2006. Function and evolution of a mosquito salivary protein family. J. Biol. Chem. 281, 1935–1942. https://doi.org/10.1074/jbc.M510359200.

Calvo, E., Mans, B.J., Ribeiro, J.M.C., Andersen, J.F., 2009. Multifunctionality and mechanism of ligand binding in a mosquito antiinflammatory protein. Proc. Natl. Acad. Sci. U.S.A. 106, 3728–3733. https://doi.org/10.1073/pnas.0813190106.

Chagas, A.C., Oliveira, F., Debrabant, A., Valenzuela, J.G., Ribeiro, J.M.C., Calvo, E., 2014. Lundep, a sand fly salivary endonuclease increases *Leishmania* parasite survival in neutrophils and inhibits XIIa contact activation in human plasma. PLoS Pathog. 10, e1003923. https://doi.org/10.1371/journal.ppat.1003923.

Charlab, R., Valenzuela, J.G., Rowton, E.D., Ribeiro, J.M.C., 1999. Toward an understanding of the biochemical and pharmacological complexity of the saliva of a hematophagous sand fly *Lutzomyia longipalpis*. Proc. Natl. Acad. Sci. 96, 15155–15160. https://doi.org/10.1073/pnas.96.26.15155.

Collin, N., Assumpcao, T.C.F., Mizurini, D.M., Gilmore, D.C., Dutra-Oliveira, A., Kotsyfakis, M., Sá-Nunes, A., Teixeira, C., Ribeiro, J.M.C., Monteiro, R.Q., Valenzuela, J.G., Francischetti, I.M.B., 2012. Lufaxin, a novel factor Xa inhibitor from the salivary gland of the sand fly *Lutzomyia longipalpis* blocks protease-activated receptor 2 activation and inhibits inflammation and thrombosis in vivo. Arterioscler. Thromb. Vasc. Biol. 32, 2185–2196. https://doi.org/10.1161/ATVBAHA.112.253906.

Coutinho-Abreu, I.V., Valenzuela, J.G., 2018. Comparative evolution of sand fly salivary protein families and implications for biomarkers of vector exposure and salivary vaccine candidates. Front. Cell. Infect. Microbiol. 8. https://doi.org/10.3389/fcimb.2018.00290.

Cox, J., Hein, M.Y., Luber, C.A., Paron, I., Nagaraj, N., Mann, M., 2014. Accurate proteome-wide label-free quantification by delayed normalization and maximal peptide ratio extraction, termed MaxLFQ. Mol. Cell. Proteom. 13, 2513–2526. https://doi.org/10.1074/mcp.m113.031591.

de Moura, T.R., Oliveira, F., Carneiro, M.W., Miranda, J.C., Clarêncio, J., Barral-Netto, M., Brodskyn, C., Barral, A., Ribeiro, J.M.C., Valenzuela, J.G., de Oliveira, C.I., 2013. Functional transcriptomics of wild-caught *Lutzomyia intermedia* salivary glands: identification of a protective salivary protein against *Leishmania braziliensis* infection. PLoS Neglected Trop. Dis. 7, e2242. https://doi.org/10.1371/journal.pntd.0002242.

Durocher, Y., Perret, S., Kamen, A., 2002. High-level and high-throughput recombinant protein production by transient transfection of suspension-growing human 293-EBNA1 cells. Nucleic Acids Res. 30, e9. https://doi.org/10.1093/nar/30.2.e9.

Dvorak, V., Shaw, J., Volf, P., 2018. Parasite biology: the vectors. In: The Leishmaniases: Old Neglected Tropical Diseases. Springer International Publishing, Cham, pp. 31–77.

Francischetti, I.M.B., 2010. Platelet aggregation inhibitors from hematophagous animals. Toxicon 56, 1130–1144. https://doi.org/10.1016/j.toxicon.2009.12.003.

Geyer, P.K., Spana, C., Corces, V.G., 1986. On the molecular mechanism of gypsy-induced mutations at the yellow locus of *Drosophila melanogaster*. EMBO J. 5, 2657–2662.

Gomes, R.B., Oliveira, F., Teixeira, C., Meneses, C., Gilmore, D.C., Elnaiem, D.E., Kamhawi, S., Valenzuela, J.G., 2012. Immunity to sand fly salivary protein LJM11 modulates host response to vector-transmitted *Leishmania* conferring ulcer-free protection. J. Investig. Dermatol. 132, 2735–2743. https://doi.org/10.1038/jid.2012.205.

Hebert, A.S., Richards, A.L., Bailey, D.J., Ulbrich, A., Coughlin, E.E., Westphall, M.S., Coon, J.J., 2014. The one hour yeast proteome. Mol. Cell. Proteom. 13, 339–347. https://doi.org/10.1074/mcp.m113.034769.

Hostomska, J., Volfova, V., Mu, J., Garfield, M., Rohousova, I., Volf, P., Valenzuela, J.G., Jochim, R.C., 2009. Analysis of salivary transcripts and antigens of the sand fly *Phlebotomus arabicus*. BMC Genomics 10, e282. https://doi.org/10.1186/1471-2164-10-282.

Jablonka, W., Kim, I.H., Alvarenga, P.H., Valenzuela, J.G., Ribeiro, J.M.C., Andersen, J.F., 2019. Functional and structural similarities of D7 proteins in the independently-evolved salivary secretions of sand flies and mosquitoes. Sci. Rep. 9, 5340. https://doi.org/10.1038/s41598-019-41848-0.

Jeffery, G.M., 1956. Blood meal volume in *Anopheles quadrimaculatus, A. albimanus* and *Aedes aegypti*. Exp. Parasitol. 5, 371–375. https://doi.org/10.1016/0014-4894(56)90021-2.

Julius, D., Basbaum, A.I., 2001. Molecular mechanisms of nociception. Nature 413, 203–210. https://doi.org/10.1038/35093019.

Kato, H., Anderson, J.M., Kamhawi, S., Oliveira, F., Lawyer, P.G., Pham, V.M., Sangare, C.S., Samake, S., Sissoko, I., Garfield, M., Sigutova, L., Volf, P., Doumbia, S., Valenzuela, J.G., 2006. High degree of conservancy among secreted salivary gland proteins from two geographically distant *Phlebotomus duboscqi* sandflies populations (Mali and Kenya). BMC Genomics 7, e226. https://doi.org/10.1186/1471-2164-7-226.

Kato, H., Jochim, R.C., Gomez, E.a., Uezato, H., Mimori, T., Korenaga, M., Sakurai, T., Katakura, K., Valenzuela, J.G., Hashiguchi, Y., 2013. Analysis of salivary gland transcripts of the sand fly *Lutzomyia ayacuchensis*, a vector of Andean-type cutaneous leishmaniasis. Infect. Genet. Evol. 13, 56–66. https://doi.org/10.1016/j.meegid.2012.08.024.

Katoh, T., Tiemeyer, M., 2013. The N's and O's of *Drosophila* glycoprotein glycobiology. Glycoconj. J. 30, 57–66. https://doi.org/10.1007/s10719-012-9442-x.

Lerner, E.A., Shoemaker, C.B., 1992. Maxadilan. Cloning and functional expression of the gene encoding this potent vasodilator peptide. J. Biol. Chem. 267, 1062–1066.

Lestinova, T., Rohousova, I., Sima, M., de Oliveira, C.I., Volf, P., 2017. Insights into the sand fly saliva: blood-feeding and immune interactions between sand flies, hosts, and *Leishmania*. PLoS Neglected Trop. Dis. 11, e0005600. https://doi.org/10.1371/journal.pntd.0005600.

Li, Z., Michael, I.P., Zhou, D., Nagy, A., Rini, J.M., 2013. Simple *piggyBac* transposon-based mammalian cell expression system for inducible protein production. Proc. Natl. Acad. Sci. 110, 5004–5009. https://doi.org/10.1073/pnas.1218620110.

Ma, D., Assumpcao, T.C.F., Li, Y., Andersen, J.F., Ribeiro, J.M.C., Francischetti, I.M.B., 2012. Triplatin, a platelet aggregation inhibitor from the salivary gland of the triatomine vector of Chagas Disease, binds to TXA2 but does not interact with glycoprotein GPVI. Thromb. Haemost. 107, 111–123. https://doi.org/10.1160/TH11-10-0685.

Mans, B.J., Ribeiro, J.M.C., 2008. Function, mechanism and evolution of the moubatin-clade of soft tick lipocalins. Insect Biochem. Mol. Biol. 38, 841–852. https://doi.org/10.1016/j.ibmb.2008.06.007.

Mans, B.J., Calvo, E., Ribeiro, J.M.C., Andersen, J.F., 2007. The crystal structure of D7r4, a salivary biogenic amine-binding protein from the malaria mosquito *Anopheles gambiae*. J. Biol. Chem. 282, 36626–36633. https://doi.org/10.1074/jbc.M706410200.

Mans, B.J., Ribeiro, J.M.C., Andersen, J.F., 2008. Structure, function, and evolution of biogenic amine-binding proteins in soft ticks. J. Biol. Chem. 283, 18721–18733. https://doi.org/10.1074/jbc.M800188200.

Marinotti, O., James, A.A., Ribeiro, J.M.C., 1990. Diet and salivation in female *Aedes aegypti* mosquitoes. J. Insect Physiol. 36, 545–548. https://doi.org/10.1016/0022-1910(90)90021-7.

Masuda, T., Tomita, M., Ishihama, Y., 2008. Phase transfer surfactant-aided trypsin digestion for membrane proteome analysis. J. Proteome Res. 7, 731–740. https://doi.org/10.1021/pr700658q.

Nascimento, E., dos Santos Malafronte, R., Marinotti, O., 2000. Salivary gland proteins of the mosquito Culex quinquefasciatus. Arch. Insect Biochem. Physiol. 43, 9–15. https://doi.org/10.1002/(SICI)1520-6327(200001)43:1<9. AID-ARCH2>3.0.CO;2-2.

Oliveira, F., Kamhawi, S., Seitz, A.E., Pham, V.M., Guigal, P.M., Fischer, L., Ward, J., Valenzuela, J.G., 2006. From transcriptome to immunome: identification of DTH inducing proteins from a *Phlebotomus ariasi* salivary gland cDNA library. Vaccine 24, 374–390. https://doi.org/10.1016/j.vaccine.2005.07.085.

Paesen, G.C., Adams, P.L., Harlos, K., Nuttall, P.A., Stuart, D.I., 1999. Tick histamine-binding proteins: isolation, cloning, and three-dimensional structure. Mol. Cell 3, 661–671. https://doi.org/10.1016/S1097-2765(00)80359-7.

Pruzinova, K., Sadlova, J., Seblova, V., Homola, M., Votypka, J., Volf, P., 2015. Comparison of bloodmeal digestion and the peritrophic matrix in four sand fly species differing in susceptibility to *Leishmania donovani*. PLoS One 10, e0128203. https://doi.org/10.1371/journal.pone.0128203.

Ribeiro, J.M.C., 1995. Blood-feeding arthropods: live syringes or invertebrate pharmacologists? Infect. Agents Dis. 4, 143–152. https://doi.org/10.1111/j.1558-5646.2010.01162.x.

Ribeiro, J.M.C., Arca, B., 2009. From sialomes to the sialoverse: an insight into salivary potion of blood-feeding insects. Adv. Insect Physiol. 37, 59–118. https://doi.org/10.1016/S0065-2806(09)37002-2.

Ribeiro, J.M.C., Francischetti, I.M.B., 2003. Role of arthropod saliva in blood feeding: Sialome and post-sialome perspectives. Annu. Rev. Entomol. 48, 73–88. https://doi.org/10.1146/annurev.ento.48.060402.102812.

Ribeiro, J.M.C., Modi, G.B., Tesh, R.B., 1989. Salivary apyrase activity of some old world phlebotomine sand flies. Insect Biochem. 19, 409–412. https://doi.org/10.1016/0020-1790(89)90046-2.

Ribeiro, J.M.C., Katz, O., Pannell, L.K., Waitumbi, J., Warburg, A., 1999. Salivary glands of the sand fly *Phlebotomus papatasi* contain pharmacologically active amounts of adenosine and 5'-AMP. J. Exp. Biol. 202, 1551–1559.

Rohousova, I., Subrahmanyam, S., Volfova, V., Mu, J., Volf, P., Valenzuela, J.G., Jochim, R.C., 2012. Salivary gland transcriptomes and proteomes of *Phlebotomus tobbi* and *Phlebotomus sergenti*, vectors of leishmaniasis. PLoS Neglected Trop. Dis. 6, e1660. https://doi.org/10.1371/journal.pntd.0001660.

Sangamnatdej, S., Paesen, G.C., Slovak, M., Nuttall, P.A., 2002. A high affinity serotonin- and histamine-binding lipocalin from tick saliva. Insect Mol. Biol. 11, 79–86. https://doi.org/10.1046/j.0962-1075.2001.00311.x.

Scheuermann, T.H., Padrick, S.B., Gardner, K.H., Brautigam, C.A., 2016. On the acquisition and analysis of microscale thermophoresis data. Anal. Biochem. 496, 79–93. https://doi.org/10.1016/j.ab.2015.12.013.

Schmitzova, J., Klaudiny, J., Albert, S., Schroder, W., Schreckengost, W., Hanes, J., Judova, J., Simuth, J., 1998. A family of major royal jelly proteins of the honeybee Apis mellifera. L. Cell. Mol. Life Sci. 54, 1020–1030. https://doi.org/10.1007/s000180050229.

Schuck, P., 2000. Size-distribution analysis of macromolecules by sedimentation velocity ultracentrifugation and Lamm equation modeling. Biophys. J. 78, 1606–1619. https://doi.org/10.1016/S0006-3495(00)76713-0.

Seidel, S.A.I., Dijkman, P.M., Lea, W.A., van den Bogaart, G., Jerabek-Willemsen, M., Lazic, A., Joseph, J.S., Srinivasan, P., Baaske, P., Simeonov, A., Katritch, I., Melo, F.A., Ladbury, J.E., Schreiber, G., Watts, A., Braun, D., Duhr, S., 2013. Microscale thermophoresis quantifies biomolecular interactions under previously challenging conditions. Methods 59, 301–315. https://doi.org/10.1016/j.ymeth.2012.12.005.

Sievers, F., Wilm, A., Dineen, D., Gibson, T.J., Karplus, K., Li, W., Lopez, R., McWilliam, H., Remmert, M., Soding, J., Thompson, J.D., Higgins, D.G., 2011. Fast, scalable generation of high-quality protein multiple sequence alignments using Clustal Omega. Mol. Syst. Biol. 7. https://doi.org/10.1038/msb.2011.75.

Sima, M., Ferencova, B., Warburg, A., Rohousova, I., Volf, P., 2016a. Recombinant salivary proteins of Phlebotomus orientalis are suitable Antigens to measure exposure of Domestic animals to sand fly bites. PLoS Neglected Trop. Dis. 10, e0004553. https://doi.org/10.1371/journal.pntd.0004553.

Sima, M., Novotny, M., Pravda, L., Sumova, P., Rohousova, I., Volf, P., 2016b. The diversity of yellow-related proteins in sand flies (Diptera: psychodidae). PLoS One 11, e0166191. https://doi.org/10.1371/journal.pone.0166191.

Sumova, P., 2019. S1 Table. The mass spectrometry analysis of *P. Perniciosus* and *P. orientalis* salivary proteins. Mendeley Data vol. 1. https://doi.org/10.17632/ryz2djytsz.1.

Sumova, P., Sima, M., Spitzova, T., Osman, M.E., Guimaraes-Costa, A.B., Oliveira, F., Elnaiem, D.-E.A., Hailu, A., Warburg, A., Valenzuela, J.G., Volf, P., 2018. Human antibody reaction against recombinant salivary proteins of *Phlebotomus orientalis* in Eastern Africa. PLoS Neglected Trop. Dis. 12, e0006981. https://doi.org/10.1371/journal.pntd.0006981.

Tyanova, S., Temu, T., Sinitcyn, P., Carlson, A., Hein, M.Y., Geiger, T., Mann, M., Cox, J., 2016. The Perseus computational platform for comprehensive analysis of (prote) omics data. Nat. Methods 13, 731–740. https://doi.org/10.1038/nmeth.3901.

Valenzuela, J.G., Garfield, M., Rowton, E.D., Pham, V.M., 2004. Identification of the most abundant secreted proteins from the salivary glands of the sand fly *Lutzomyia longipalpis*, vector of *Leishmania chagasi*. J. Exp. Biol. 207, 3717–3729. https://doi.org/10.1242/jeb.01185.

Velez, R., Spitzova, T., Domenech, E., Willen, L., Cairo, J., Volf, P., Gallego, M., 2018. Seasonal dynamics of canine antibody response to *Phlebotomus perniciosus* saliva in an endemic area of *Leishmania infantum*. Parasit. Vectors 11, e545. https://doi.org/10.1186/s13071-018-3123-y.

Vlkova, M., Sima, M., Rohousova, I., Kostalova, T., Sumova, P., Volfova, V., Jaske, E.L., Barbian, K.D., Gebre-Michael, T., Hailu, A., Warburg, A., Ribeiro, J.M.C., Valenzuela, J.G., Jochim, R.C., Volf, P., 2014. Comparative analysis of salivary gland transcriptomes of *Phlebotomus orientalis* sand flies from endemic and non-endemic foci of visceral leishmaniasis. PLoS Neglected Trop. Dis. 8, e2709. https://doi.org/10.1371/journal.pntd.0002709.

Volf, P., Skarupova, S., Man, P., 2002. Characterization of the lectin from females of *Phlebotomus duboscqi* sand flies. Eur. J. Biochem. 269, 6294–6301. https://doi.org/10.1046/j.1432-1033.2002.03349.x.

Volfova, V., Volf, P., 2018. The salivary hyaluronidase and apyrase of the sand fly *Sergentomyia* (Diptera, *Psychodidae*). Insect Biochem. Mol. Biol. 102, 67–74. https://doi.org/10.1016/j.ibmb.2018.09.010.

Volfova, V., Hostomska, J., Cerny, M., Votypka, J., Volf, P., 2008. Hyaluronidase of bloodsucking insects and its enhancing effect on *Leishmania infection* in mice. PLoS Neglected Trop. Dis. 2, e294. https://doi.org/10.1371/journal.pntd.0000294.

Wienken, C.J., Baaske, P., Rothbauer, U., Braun, D., Duhr, S., 2010. Protein-binding assays in biological liquids using microscale thermophoresis. Nat. Commun. 1. https://doi.org/10.1038/ncomms1093.

Xanthos, D.N., Bennett, G.J., Coderre, T.J., 2008. Norepinephrine-induced nociception and vasoconstrictor hypersensitivity in rats with chronic post-ischemia pain. Pain 137, 640–651. https://doi.org/10.1016/j.pain.2007.10.031.

Xu, X., Oliveira, F., Chang, B.W., Collin, N., Gomes, R., Teixeira, C., Reynoso, D., Pham, V.M., Elnaiem, D.-E., Kamhawi, S., Ribeiro, J.M.C., Valenzuela, J.G., Andersen, J.F., 2011. Structure and function of a "yellow" protein from saliva of the sand fly *Lutzomyia longipalpis* that confers protective immunity against *Leishmania major* infection. J. Biol. Chem. 286, 32383–32393. https://doi.org/10.1074/jbc.M111.268904.

Xu, X., Chang, B.W., Mans, B.J., Ribeiro, J.M.C., Andersen, J.F., 2013. Structure and ligand-binding properties of the biogenic amine-binding protein from the saliva of a blood-feeding insect vector of *Trypanosoma cruzi*. Acta Crystallogr. Sect. D Biol. Crystallogr. 69, 105–113. https://doi.org/10.1107/S0907444912043326.

Yosipovitch, G., Rosen, J.D., Hashimoto, T., 2018. Itch: from mechanism to (novel) therapeutic approaches. J. Allergy Clin. Immunol. 142, 1375–1390. https://doi.org/10.1016/j.jaci.2018.09.005.